PERGAMON

Computers in Biology and Medicine 28 (1998) 143–152

Computers in Biology and Medicine

Generation and characterization of correlated spike trains

D.M. Halliday *

Division of Neuroscience and Biomedical Systems, West Medical Building, University of Glasgow, Glasgow G12 8QQ, UK

Received 10 October 1997

Abstract

A framework within which to generate and characterize populations of correlated spike trains is presented. Spike trains are generated using integrate to threshold and fire type encoders. Spectral analysis techniques form the basis for specifying the strength of correlation within the population. To accurately specify weak correlation, a combined coherence estimate is formed between several independent pairs of spike trains from a population. The aim is to produce populations of spike trains which have a realistic stochastic correlation structure and which can be used to explore the role of correlated neuronal discharge in information processing in neuronal systems.

Keywords: Spike trains; Coherence; Correlation; Synchronization; Simulation; Neural modelling

1. Introduction

The role of correlated neuronal discharges in transmitting information and information processing in neuronal systems is currently of considerable interest [1, 2]. The importance of models which can be used to investigate neural function is also recognised [3, 4], these models can incorporate detailed biophysical data at the single cell level. The present report is concerned with the related questions of generating and characterizing populations of spike train discharges which have a pre-specified correlation structure between pairs of spike trains within the population. The emphasis is on computational efficiency and generation of weakly correlated spike trains, which can be input to detailed single/multiple cell models to explore the role of correlated neuronal discharges in information transmission and processing in neuronal systems.

* Tel.: +44-141-330-4759; Fax: +44-141-330-4100; E-mail: gpaa34@udcf.gla.ac.uk.

0010-4825/98/$19.00
PII: S0010-4825(98)00003-1

The basic building block is the integrate to threshold and fire type encoder which incorporates a time constant [5], also known as a leaky integrator. Each spike train is generated by one such encoder and these encoders are acted upon by common inputs which are used to induce the desired patterns of correlation. Spectral analysis techniques are used to characterize the strength of correlation within the resulting population of spike trains. To accurately characterize the weak correlation, a single combined coherence estimate between several independent pairs of spike trains is formed.

2. Description of spike generators

The basic construction of each spike generator is that of an integrate to threshold and fire model. The models in the present study incorporate a first order time constant. These can be considered as part of the general class of sigma pulse frequency modulation systems (ΣPFM) described in Pavildis and Jury [5]. If we denote as x the sum of all the inputs acting on an encoder and v the output of the encoder, then the encoder can be described by the differential equation

$$\frac{\mathrm{d}\nu}{\mathrm{d}t} = \frac{G}{\tau}x - \frac{1}{\tau}\nu \tag{1}$$

where G is the gain of the encoder and τ is the time constant. The simplest method of advancing Eq. (1) through time is to use a forward Euler integration scheme. We can write this in the form of a difference equation as $v_{n+1} = v_n + \mathrm{h}\, \mathrm{d}v_n/\mathrm{d}t$, where v_{n+1} is the new value of the encoder output after advancing the encoder by a single time step, of duration h, from the value at v_n. If we use a value of 1.0 for the encoder gain and combine the above difference equation with Eq. (1) we obtain

$$\nu_{n+1} = \frac{\nu_n + h/\tau x_n}{1 + h/\tau} \tag{2}$$

to obtain the solution of Eq. (1). The new value of the encoder output can be compared with the threshold value, v_{th}. If this is exceeded, an output spike is signalled and the encoder output v is reset. If spike timings on a more precise time scale are required these can be approximated as follows. If the new voltage value, v_{n+1}, exceeds the threshold, v_{th}, the timing of threshold crossing can be estimated using a simple linear interpolation as:

$$t_n + \frac{\nu_{\mathrm{th}} - \nu_n}{\nu_{n+1} - \nu_n},$$

where t_n is the time associated with the encoder output v_n. Using this approach, the encoder firing times can be approximated on a finer time scale, without the extra burden of evaluating v_{n+1} using smaller time steps. A further refinement of this approximation would be to shift the encoder output down by v_{th} after each output spike, rather than resetting the value to zero: $v_{n+1} = v_{n+1} - v_{\mathrm{th}}$. This preserves the extra excitation provided by the inputs which is over and above that required to cross threshold.

3. Choice of parameters

Once the basic parameters have been chosen, the encoder behaviour is governed by the form of the input sequence, x. In the present study, we fix the threshold value, $v_{th} = 1.0$, and the starting value, $v_0 = 0.0$. We use a value of 10^{-3} s for h (1.0 ms) and a time constant τ of 2.5e − 02 s (25 ms).

The input sequence x for each encoder consists of two parts, an independent part which is unique to each encoder, and one or more parts which are common to all the encoders in each set. For the independent inputs we use a normal distribution. Thus, if x consists of samples from a normal distribution with a mean of 1.02 and a standard deviation (S.D.) of 0.065, each encoder will generate a spike train with a mean rate of 10.0 spikes/s and a coefficient of variation (c.o.v.) of 0.1. Altering the form of the input to have a mean of 1.015 and an S.D. of 0.15 results in generated spike trains with a mean rate of 10.0 spikes/s and a c.o.v. of 0.2. The generation of spike trains with higher mean rates is achieved by increasing the mean value of the input x. For example, input sequences with a mean value and S.D. of 1.269 and 0.307,

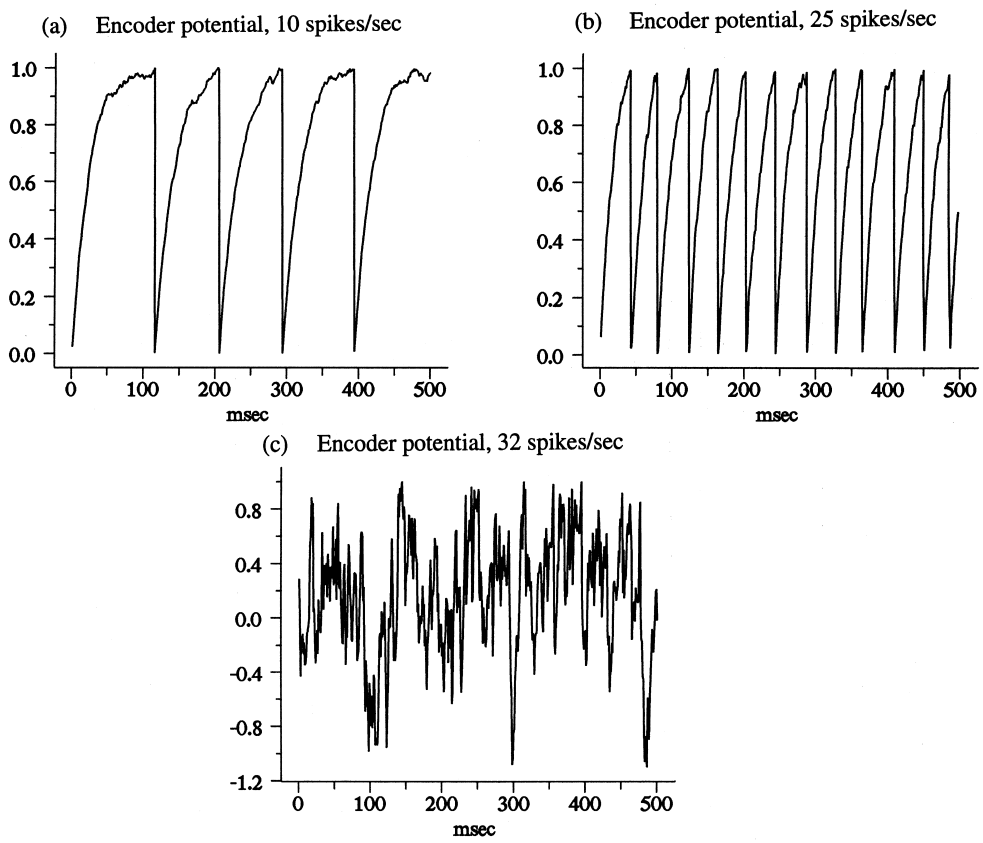

Fig. 1. Sample records of spike encoder output, including resetting after each output spike, for an average output rate and c.o.v. of (a) 10 spikes/s and 0.2, (b) 25 spikes/s and 0.1, (c) 32 spikes/s and 1.0. The last example contains 19 threshold crossings in the 500 ms segment illustrated.

respectively, result in output spike trains with mean rates and c.o.v. values of 25.0 and 0.1, respectively. It is also possible to generate random spike trains using these encoders. Inputting a sequence x with a mean of 0.892 and an S.D. of 6.20 results in generated spike trains with mean rates of 32.0 spikes/s and a c.o.v. of 1.0. In Fig. 1 are shown three examples of the encoder output, obtained from Eq. (2), for different input sequences, x. These include the resetting of the encoder each time threshold is crossed. The three examples are for (a) an output spike train with a mean rate of 10.0 spikes/s and c.o.v. of 0.2, (b) an output spike train with a mean rate of 25.0 spikes/s and c.o.v. of 0.1 and (c) an output spike train with a mean rate of 32.0 spikes/s and c.o.v. of 1.0. The timings of the output spikes can be clearly seen for the two periodic discharges.

The generation of populations of correlated spike trains involves a similar procedure, except that the input sequence x to each encoder in the population includes one or more common components, the objective of which is to induce synchronized firing among the members of the population. In the present implementation, this is achieved by the addition of pulse inputs to each input sequence x. These inputs act to increase the values of v in each encoder and for those encoders which are close to threshold will cause synchronized firing.

The step response of the first order system described in Eq. (1) to rectangular pulse inputs is well known, e.g. Ref. [6]. It is described by an exponential function, whose form is determined by the characteristics of the pulse and the time constant of the encoder. The magnitude of the encoder response to pulse inputs can be adjusted by altering the magnitude of the pulse input and the pulse width. For example, if the input x has the form of a rectangular pulse of width 2 ms and magnitude 0.398 the response of the above encoder ($G = 1.0$, $\tau = 25$ ms) will increase by 0.03 after 2 ms. If the magnitude of the pulse is increased to 1.33, the encoder response will have increased by 0.1 after 2 ms. In this way the desired strength of correlation can be obtained within the population of spike generators. The frequency of correlation can be determined by the inter spike interval distribution of these common pulse inputs to the spike generators.

4. Specification of correlation strength

To describe accurately the strength of correlation within the population of spike trains requires an analytical framework which can estimate the strength of correlation between spike trains. Spectral analysis provides such a framework, in particular we use estimates of coherence functions to describe the strength of correlation between pairs of spike trains. In the present report, we adopt the framework of Halliday et al. [7]. The generated spike train data are assumed to be realisations of stationary stochastic point-process data. A stochastic point-process can be defined formally as a non-negative integer valued measure [8], which in practice defines the ordered times of occurrence of spikes in terms of a multiple of the sampling interval (1 ms). The coherence function between two spike trains a and b, at frequency λ, $|R_{ab}(\lambda)|^2$, can be defined as

$$|R_{ab}(\lambda)|^2 = \frac{|f_{ab}(\lambda)|^2}{f_{aa}(\lambda) f_{bb}(\lambda)} \tag{3}$$

where $f_{aa}(\lambda)$ and $f_{bb}(\lambda)$ are the autospectra of spike trains a and b, respectively, and $f_{ab}(\lambda)$ is the cross spectrum. An estimation procedure follows directly from Eq. (3) by direct substitution of spectral estimates. In the present study we use the spectral estimation technique described in Ref. [7], where the complete record is broken down into a number of non-overlapping disjoint sections of equal length and stable spectral estimates are obtained by averaging across the sections. This approach also allows significance levels to be determined by a simple expression, which depends only on the number of disjoint sections. In this case a 95% confidence limit for estimates of the coherence function, under the assumption of independent spike trains, is given by the expression $1-(0.05)^{1/(L-1)}$, where L is the number of disjoint sections [7]. If tapering is used to form the spectral estimates, then this expression must be adjusted accordingly to reflect the increased variance [9].

It is also possible to characterize the correlation between two spike trains as a function of time. In the present report we use estimates of the cumulant density function, denoted by $q_{ab}(u)$ at time lag u. This is defined and estimated as the inverse Fourier transform of the cross spectrum, $f_{ab}(\lambda)$ [7].

One complication we are faced with in the present study is the specification of weak correlations. In cases where the strength of correlation is of the same order as the significance level for a single record, an accurate estimate of the correlation strength is not possible. This problem can be overcome using the technique of pooled coherence [10]. This estimates a single pooled coherence from several records in the form of a weighted average. The increase in the amount of data used to estimate the pooled coherence function results in reduced standard errors, which provides a more accurate estimate of the average strength of correlation between pairs of spike trains from a single population. In summary, if we have k pairs of spike trains: a_i, b_i; $i = 1, \ldots, k$; then the pooled coherence can be defined as

$$\left(\left|\sum_{i=1}^{k} f_{a_i b_i}(\lambda) L_i\right|^2\right)\left(\left(\sum_{i=1}^{k} f_{a_i a_i}(\lambda) L_i\right)\left(\sum_{i=1}^{k} f_{b_i b_i}(\lambda) L_i\right)\right)^{-1} \tag{4}$$

where L_i is the number of disjoint sections used to estimate the auto spectra, $f_{a_i a_i}(\lambda)$ and $f_{b_i b_i}(\lambda)$, and the cross spectra, $f_{a_i b_i}(\lambda)$, for the ith record. The upper 95% confidence limit for the pooled coherence, Eq. (4), under the assumption of independence can be approximated by the value $1-(0.05)^{1/(\Sigma L_i - 1)}$, where ΣL_i is the total number of segments in the pooled coherence estimate [10]. We take advantage of the fact that coherence and pooled coherence functions provide a normative measure of linear association, on a scale from 0 to 1, and have similar interpretations, to compare the strength of correlation between different populations of correlated spike trains.

5. Examples

The first example consists of a population of periodically firing spike trains which are weakly correlated at the frequency corresponding to the mean firing rate. The desired firing rate for each spike generator is 10 spikes/s, with a c.o.v. of 0.1. The two components of the input, x, to each encoder are (1) an independent component of samples from a normal distribution with a

mean of 1.018 and an S.D. of 0.065 and (2) a common component of pulses of magnitude 0.0928 and width 2 ms triggered by the times of a single spike train which has the same inter spike interval statistics as those for each spike generator, 10 spikes/s and c.o.v. 0.1. Each pulse increases v towards the threshold by 0.007 in each encoder. A sample set of 100 spike trains of duration 100 s with these characteristics was generated and subjected to the above analysis.

Shown in Fig. 2(a) is the estimated point process autospectrum of the discharge of one spike train. All spectral estimates in this report have a segment length of 1024 points, equivalent to 1.024 s, which defines the spectral resolution as 0.98 Hz. The fundamental component at the frequency of 10 Hz, corresponding to the discharge rate, can clearly be seen along with harmonic components. In Fig. 2(b) and (c) are shown estimates of the cumulant density function and coherence function for a single pair of spike trains from the population. The cumulant has a small peak at time zero, which exceeds the upper 95% confidence limit, and which indicates a tendency for synchronized discharge. The coherence estimate has significant

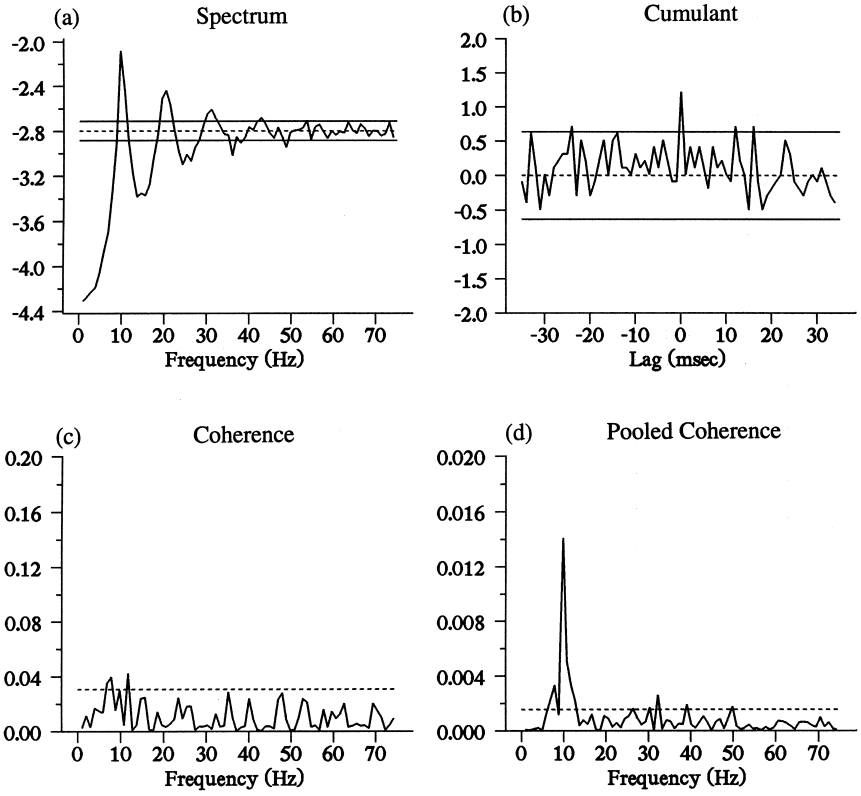

Fig. 2. Analysis of periodic spike trains correlated at 10 Hz, the desired firing rate is 10 spikes/s, with a c.o.v. of 0.1. (a) Estimated autospectrum of one discharge, dashed and solid horizontal lines are expected value and upper and lower 95% confidence limits, respectively, based on the assumption of a Poisson spike train. (b) Estimated cumulant density and (c) estimated coherence between one pair of discharges. (d) Estimated pooled coherence between 20 independent pairs of such discharges. Dashed and solid horizontal lines in (b, c, d) are upper 95% confidence limits based on assumption of independence.

values around 10 Hz. However, it is difficult to determine accurately that the two spike trains are correlated at 10 Hz. Indeed, in a sample of 50 pairs of spike trains from this population, the majority of individual pairs exhibit no significant features in coherence or cumulant density estimates. To specify more accurately the correlation within this population of spike trains the pooled coherence estimate formed from a total of 20 pairs is shown in Fig. 2(d). This estimate is constructed from a total of 1940 segments ($L_i = 97$, $i = 1, \ldots, 20$), the estimated upper 95% confidence limit of 0.0015 allows the weak correlation within the population of spike trains to be more accurately specified than from a single record. The estimated peak coherence value of around 0.015 indicates that the strength of correlation within the population is extremely weak.

In the second example we consider a population of correlated spike trains which have a random discharge pattern, i.e. the individual spike trains in the population have a c.o.v. of around 1.0. The desired firing rate in this case is 32 spikes/s. The independent components of the input, x, to each encoder are samples from a normal distribution with a mean of 0.523 and S.D. of 6.30. Each encoder is acted upon by two common components, one at 10 Hz and another at 25 Hz. The common input at 10 Hz is activated by a single spike train of rate 10 spikes/s and c.o.v. of 0.1, which adds a pulse input of width 2 ms and magnitude 6.63 to the input, x, of each encoder. The effect of this component is to increase the encoder output, v, by 0.5 towards threshold. The second common component at 25 Hz is activated by a single spike train of rate 25 spikes/s and c.o.v. of 0.1, which adds a pulse input of width 2 ms and magnitude 3.98 to each encoder input, the effect of which is to increase the encoder output, v, by 0.3 towards threshold. The estimated autospectrum of one discharge from the population is shown in Fig. 3(a). The record length is 100 s as in the previous example. The mean rate and c.o.v. of this spike train are 32.4 spikes/s and 1.0. The spectrum is flat as expected, but does deviate slightly from the expected value for that of a Poisson spike train of the same mean rate (horizontal dashed line), reflecting the finite dead time of the spike encoder. There is no indication in the power spectrum of distinct components at 10 or 25 Hz. As in the previous example, the correlation between a single pair of spike trains fails to reveal the correct correlation structure in either the time domain, Fig. 3(b), or the frequency domain, Fig. 3(c). The pooled coherence estimate, constructed as above from 20 different pairs of discharges from the population, does reveal that the spike trains are correlated at 10 and 25 Hz. In this case the peak values of the estimated pooled coherence are around 0.03 and 0.025, and indicate that the correlation within the population is weak, and that it is stronger than the previous example.

6. Discussion

In the present report we have set out a framework within which to generate and characterize weakly correlated spike trains. For the spike encoders, the emphasis has been on simplicity and computational efficiency. The problems with a forward Euler integration scheme are well known [11], i.e. instability and inaccuracy. Since we are not interested in accurate solutions of Eq. (1) this scheme is adequate for our purposes. Stability is not a problem for the range of firing rates considered in the present study, a 1 ms time step gives stable behaviour, even for the generation of random spike trains. The choice of time constant is determined by several factors. Without any time constant there is no memory in the encoders which results in

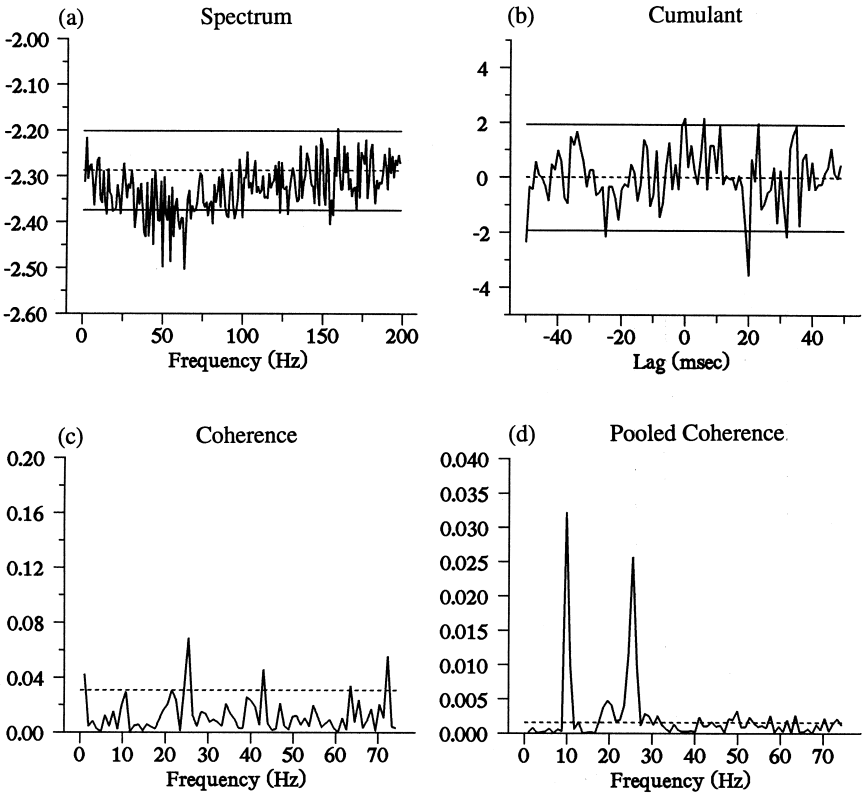

Fig. 3. Analysis of random spike trains correlated at 10 and 25 Hz, the desired firing rate is 32 spikes/s, with a c.o.v. of 1.0. (a) Estimated autospectrum of one discharge, dashed and solid horizontal lines are expected value and upper and lower 95% confidence limits, respectively, based on the assumption of a Poisson spike train. (b) Estimated cumulant density and (c) estimated coherence between one pair of discharges. (d) Estimated pooled coherence between 20 independent pairs of such discharges. Dashed and solid horizontal lines in (b, c, d) are upper 95% confidence limits based on assumption of independence.

correlated spike trains which are tightly coupled in time. With a large time constant the response of the encoders is too slow to generate correlated spike trains at the frequencies of interest. With a short time constant, of the order of the integration step size h, the encoders respond rapidly to small inputs, and considerations of stability and integration errors then become important. The value of $\tau = 25$ ms used allows correlated spike trains to be effectively and efficiently generated at the frequencies of interest. Both examples above required around 110 s of computer time on a 486/66 PC and around 15 s on a DEC Alpha EB164/300. These times include running all the encoders for 2000 steps to randomize the starting point of each encoder, otherwise all the encoders start from $v = 0.0$ and are tightly synchronized for the first few output spikes.

Pulse frequency modulation techniques have been widely used to simulate neural systems, e.g. Ref. [12]. It is not our intention to simulate neural behaviour, rather to use their cell like properties (integrate to threshold and fire) to efficiently generate spike trains with particular characteristics.

Two previous studies have explored the effects of synchronized inputs on the output firing rate of single neurones. Murthy and Fetz [13] generated simulated inputs by lumping multiple inputs into a single input whose strength increased proportionally. Bernander et al. [14] used inputs where a fixed fraction of the inputs fired within a narrow time window to simulated correlated inputs. Both these studies concluded that synchronized inputs could exert an influence of the output firing rate of the post-synaptic cell. The techniques presented in the present report provide a basis from which to extend these studies by allowing the generation of correlated spike trains with patterns of correlation which match more closely the stochastic nature of neuronal discharges [15], as opposed to the deterministic form of correlation used by the above authors. The role of rhythmically synchronized inputs of varying strength and frequencies of synchronization can also be explored in detail with the techniques presented.

We finish by speculating on a possible corollary to the second example, which demonstrated that a population of apparently random spike trains, characterized by a c.o.v. ~ 1.0, can be weakly synchronized in different frequency bands and that a statistical analysis of a single sample record of 100 s duration can fail to reveal this synchronization. Softky and Koch [16] found that the responses of individual cortical neurones to visual stimuli were characterized by irregular spike trains with a c.o.v. ~ 1.0 and that this variability could not be explained by temporal summation in passive dendrites of randomly timed EPSPs. Using computer simulations they postulated that this high inter-spike interval variability could be explained by including active dendritic conductances, which changed the response of the cell to that of a coincidence detector. The above techniques provide the means to explore another aspect of this variable firing in cortical cells, namely that a large population of randomly firing inputs spike trains which are weakly correlated could contribute to the output firing variability.

7. Summary

A framework for the generation and characterization of populations of correlated spike trains is presented. The spike trains are generated using integrate to threshold and fire type encoders, the correlation is induced by applying common pulse inputs to these encoders. The correlation structure is characterized using spectral analysis techniques, in particular coherence estimates between pairs of spike trains from the population are used to estimate the strength of correlation between sample pairs of spike trains. To characterize weak correlation we construct a combined coherence estimate formed as a weighted average between several pairs, the reduced standard errors of this estimate allows weak correlation to be accurately specified. Two examples are presented, the first is a population of periodic spike trains which is correlated at the frequency of firing, the second is a population of randomly firing spike trains (with a coefficient of variation of 1.0) which are correlated at two different frequencies. The aim is to allow the generation of populations of spike trains, which have a correlation structure that matches the stochastic nature of neuronal discharges, and which can be input to detailed biophysical neuronal models to explore the role of correlated synchronous neuronal discharges in information processing in neuronal systems.

Acknowledgements

Supported by The Wellcome Trust (036928; 048128) and the Joint Research Council/HCI Cognitive Science Initiative.

References

[1] W. Singer, Synchronization of cortical activity and its putative role in information processing and learning, Ann. Rev. Physiol. 55 (1993) 349–374.
[2] C.M. Gray, Synchronous oscillations in neuronal systems: Mechanisms and functions, J. Comput. Neurosci. 1 (1994) 11–38.
[3] T.J. Sejnowski, The year of the dendrite, Science 275 (1997) 178–179.
[4] C. Koch, Computation and the single neuron, Nature 385 (1997) 207–210.
[5] T. Pavildis, E.I. Jury, Analysis of a new class of pulse frequency modulated feedback systems, IEEE Trans. Automatic Control 10 (1965) 35–43.
[6] R.C. Dorf, Modern Control Systems, 3rd ed., Addison-Wesley, 1980, p. 493.
[7] D.M. Halliday, J. R Rosenberg, A.M. Amjad, P. Breeze, B.A. Conway, S.F. Farmer, A framework for the analysis of mixed time series/point process data: theory and application to the study of physiological tremor, single motor unit discharges and electromyograms, Prog. Biophys. Mol. Biol. 64 (1995) 237–278.
[8] D.R. Brillinger, Comparative aspects of the study of ordinary time series and of point processes, in: P.R. Krishnaiah (Ed.), Developments in Statistics, Vol. 1, Academic Press, New York, 1978, pp. 33–133.
[9] D.R. Brillinger, Time Series: Data Analysis and Theory, 2nd ed., Holden Day, San Francisco, 1981.
[10] A.M. Amjad, D.M. Halliday, J.R. Rosenberg, B.A. Conway, An extended difference of coherence test for comparing and combining independent estimates: theory and application to the study of motor units and physiological tremor, J. Neurosci. Methods 73 (1997) 69–79.
[11] S.D. Conte, C. de Boor, Elementary Numerical Analysis. An Algorithmic Approach, McGraw-Hill, 1981, p. 432.
[12] B. Knight, Dynamics of encoding in a population of neurons, J. Gen. Physiol. 59 (1972) 734–766.
[13] V.N. Murthy, E.E. Fetz, Effects of input synchrony on the firing rate of a three conductance cortical neuron model, Neural Comput. 6 (1994) 1111–1126.
[14] BernanderÖ., C. Koch, M. Usher, The effect of synchronized inputs at the single neuron level, Neural Comput. 6 (1994) 622–641.
[15] A.V. Holden, Models of the Stochastic Activity of Neurones. Lecture Notes in Biomathematics, vol. 12, Springer-Verlag, 1976, p. 368.
[16] W.R. Softky, C. Koch, The highly irregular firing of cortical cells is inconsistent with temporal integration of random EPSPs, J. Neurosci. 13 (1993) 334–350.